Vegetation index-based partitioning of evapotranspiration is deficient in disturbed systems

Pushpendra Raghav[1], Pradeep Wagle[2], Mukesh Kumar[1], Tirtha Banerjee[3], James P.S. Neel[2]

[1]Department of Civil, Construction, and Environmental Engineering, University of Alabama, Tuscaloosa, AL, USA
[2]USDA, Agricultural Research Service, Grazinglands Research Laboratory, El Reno, OK, USA
[3]Department of Civil and Environmental Engineering, University of California, Irvine, CA, 92697, USA

Key Points:

- Three Evapotranspiration (ET) partitioning methods were used to partition ET in differently managed wheat systems
- Grazing altered the relation between transpiration:ET and enhanced vegetation index
- ET partitioning errors were higher in disturbed (i.e., grazed) systems

Corresponding author: Mukesh Kumar, `mkumar4@eng.ua.edu`

Abstract

Partitioning evapotranspiration (ET) into its primary components, i.e., evaporation (E) and plant transpiration (T), is needed in a range of hydrometeorological applications. Using vegetation index (VI) to obtain spatially resolved T:ET ratio over large areas has emerged as a promising approach in this regard. Here, we assess the effectiveness of this approach in differently managed wheat systems. Results show a weak relation between T:ET and VI in disturbed (i.e., grazed) systems. Flux partitions based on a canonical T:ET vs. VI relation or one derived in a neighboring undisturbed wheat system introduce large errors in disturbed systems, thus underscoring the limits on the transferability of the VI-based ET partitioning approach. The effectiveness of the VI-based approach is found to be related to the strength of correlation between VI and vapor pressure deficit and/or radiation. This correlation metric can help identify settings where the approach is likely to be effective.

Plain Language Summary

Evapotranspiration (ET) plays a significant role in water and climate cycles by affecting the energy and water balance over the land surface which in turn mediates the land-atmosphere interactions. ET is composed of two primary components i.e., direct evaporation (E) and plant transpiration (T). Partitioning total ET into its individual components (E and T) is of significant importance for better assessment of both regional and global water budgets. One of the primary approaches to partition ET over large areas is by using vegetation indices (VI), which indirectly capture plants' biophysical state. This approach has been used to partition ET in different landscapes, but its efficacy has not been tested in disturbed ecosystems, which cover a large fraction of earth's vegetated area. Here, we assess the effectiveness of this VI-based ET partitioning approach in disturbed (i.e., grazed) ecosystems. We find that the VI-based ET partitioning introduces large errors in disturbed systems. Further investigation identifies conditions that can be used to filter-out regions where the VI-based partition is likely to be more (or less) effective.

1 Introduction

Around 60% of the precipitated water is returned to the atmosphere by evapotranspiration (ET) (Oki & Kanae, 2006). Unsurprisingly, ET plays a major role in influencing the water and climate cycles components at both local and global scales (Jung et al., 2010; Zhang et al., 2016; Condon & Maxwell, 2019; R. Wang et al., 2013; Oishi et al., 2010; Bonetti et al., 2015). To assess these influences, it is crucial to partition ET into its components, viz. evaporation (E) from bare soil and wet plant surfaces, and plant transpiration (T). This is especially needed as relative contributions of E and T vary in space and time, in part due to the varied controls on E and T (Ritchie & Burnett, 1971; Unkovich et al., 2018). For instance, in addition to the meteorological, soil, and plant morphometric properties that influence E, T is also majorly influenced by plant physiology (H. Wang & Liu, 2007; X. Sun et al., 2019; Liu et al., 2017, 2020). Partitioning of ET can facilitate understanding of plants' water use strategies and their responses to environmental forcings, help assess the role of changes in land cover on ET, and improve predictions of hydrological responses as moisture used for E and T are usually derived from different soil stores (Perez-Priego et al., 2018; Zeng et al., 2017; Alkama & Cescatti, 2016; X. Chen et al., 2015).

Over the past years, several methods have been developed for ET partitioning to improve our understanding of the dynamics of T over ET (T:ET hereafter). Details on the various methods of partitioning of eddy covariance (EC) measured ET and their challenges are well documented elsewhere (Kool et al., 2014; Stoy et al., 2019). Majority of the methods provide T:ET estimates at the gauging sites (e.g., (Zhou et al., 2016; Scanlon & Sahu, 2008; Perez-Priego et al., 2018; Nelson et al., 2020; Scott & Biederman, 2017; Li et al., 2019; Paul-Limoges et al., 2020; Black et al., 1969)) or over its flow contribution area (e.g., (Jasechko et al., 2013; Good et al., 2015)). To obtain spatially-explicit estimates of T:ET, numerous alternative methods have been developed. For example, Long and Singh (2012) and Zhang et al. (2019) used a remote sensing approach to partition ET. Land surface modeling (e.g., (Dirmeyer et al., 2006; Haddeland et al., 2011; Fatichi & Pappas, 2017; Paschalis et al., 2018; Lian et al., 2018)) and hybrid approaches (e.g., (Miralles et al., 2011; Martens et al., 2017)) have also been used to obtain T:ET estimates over large areas. Recently, parsimonious models that only use widely available vegetation indices to obtain T:ET at multiple temporal scales (e.g., weekly, monthly, seasonal) has received significant attention (e.g., (Berkelhammer et al., 2016; Fatichi & Pappas, 2017; L. Wang et al., 2014; Wei et al., 2015, 2017; S. Kang et al., 2003)). These models are able to explain a significant fraction of variability in T:ET using vegetation indices such as Leaf Area Index (LAI) and Enhanced Vegetation Index (EVI). For example, based on a meta-analysis, Wei et al. (2017) reported that T:ET can be well represented as a function of LAI ($R^2 = 0.87$) in cropland settings. Zhou et al. (2016) showed that T:ET is strongly related to EVI ($R^2 = 0.85$) at 8-day scale based on the concept of underlying Water Use Efficiency (uWUE). S. Kang et al. (2003) also reported a close relation between T:ET and LAI ($R^2 = 0.97$) in a winter wheat system based on lysimeter data. L. Wang et al. (2014) concluded that LAI and growth stage function can be used to obtain global T:ET estimates.

Notably, the efficacy of this approach has not been tested in disturbed ecosystems or ecosystems that experience impulse alterations in canopy cover, such as due to grazing management, thinning, hurricanes, and wildfires. Here, we furnish this gap by evaluating the relation between T:ET and vegetation index in both undisturbed and disturbed wheat systems. Here, the disturbance is introduced due to grazing management. In addition, we assess the conditions that facilitate a stronger correlation between T:ET and vegetation index. The paper is organized as follows: Section 2 provides a detailed description on the materials and methods used in this study. Results on the flux partitioning are presented in section 3.1. Section 3.2 presents the results on the relationships between T:ET and EVI. The errors statistics in the prediction of T:ET using EVI at different time scales are presented in section 3.3. Section 4.4 evaluates the controls on T:ET vs. vegetation index relation.

2 Materials and Methods

2.1 Study Sites

Two years of data from three neighboring, but differently managed, winter wheat cropping fields (Sites 1-3 hereafter) were used (Figures 1 and S1). Each field (cropped area ranging from ∼13 ha - 22 ha) had identical soil type, experienced similar climatology, and the wheat seeds were sown at about 19 cm row spacing in each field. These fields are part of the United States Department of Agriculture, Agricultural Research Service, Grazinglands Research Laboratory's flux network (GRL-FLUXNET), which is a dense network of 16 Eddy Covariance (EC) towers in central Oklahoma (El Reno), USA. During the 2016-17 growing season (October 2016 - May 2017), grain-only and graze-grain wheat were grown at sites 1 and 3, respectively. Grain-only wheat has a single purpose to produce wheat grains, while graze-grain wheat has a dual purpose as it serves as a pasture for grazing cattle from November to February and is used for producing wheat grains thereafter. As data of differently managed configurations are only available for wheat, we restrict this study to wheat crops. Hence, 2016-17 data from site 2, where Canola was grown, was not considered. In the 2017-18 growing season, site 1 had graze-grain wheat, site 2 had grain-only wheat, and site 3 had graze-out wheat. Graze-out is also a single purpose crop that is grown to solely serve as a pasture for the grazing cattle. The 2017-18 growing season data from all three sites were used for analyses.

2.2 Data

2.2.1 Eddy Covariance and Ancillary Hydro-meteorological Data

Water vapor and carbon dioxide fluxes were measured in all three wheat fields for the 2016-17 and 2017-18 growing seasons using eddy covariance (EC) systems. The data were recorded at 10 Hz frequency (i.e., 10 measurements per second) and then processed in the EddyPro software to get good quality estimates of latent heat fluxes at 30 minute intervals. More details on the EC data collection and processing can be found in Wagle et al. (2018, 2019).

Ancillary hydro-meteorological variables such as net radiation, soil water content (∼5 cm depth), air temperature, soil heat flux, soil temperature, relative humidity, incoming photosynthetic photon flux density, and infrared surface temperature were also measured at the sites. We obtained rainfall data from the Oklahoma El Reno Mesonet station (located within 1-1.5 km from the study sites).

2.2.2 Remote-sensing data

The EVI for the three differently managed wheat systems, i.e., grain-only, graze-grain, and graze-out, were derived (Figure S2) using the Landsat surface reflectance images obtained from the U.S. Geological Survey (USGS) Earth Explorer. The average EVI for each field was calculated following Jiang et al. (2008):

$$EVI = \frac{G \cdot (NIR - R)}{NIR + C1 \cdot R - C2 \cdot B + L} \tag{1}$$

where G (=2.5) is a gain factor. C1 (=6) and C2 (=7.5) are band-specific correction coefficients of aerosol resistance term. L (=1) is background brightness correction factor. NIR, R, and B are the near-infrared, red, and blue bands, respectively.

2.3 ET Partitioning

Total ET was partitioned into T and E based on three methods using the EC data sets: Flux Variance Similarity (FVS) theory-based method (Scanlon & Sahu, 2008), the underlying Water Use Efficiency (uWUE) method (Zhou et al., 2016), and the Transpiration Estimation Algorithm (TEA) method (Nelson et al., 2018). Consideration of multiple methods for this study was driven by the fact that estimates from no one method is generally considered perfect, and each of them are affected by inherent assumptions in them.

The FVS method can simultaneously partition ET and net ecosystem CO_2 exchange (NEE) into their primary components, i.e., T and E for ET, and photosynthesis and respiration for NEE, based on the correlation between high-frequency EC measurements of carbon dioxide and water vapor fluxes along with measured or estimated leaf-scale Water Use Efficiency (WUE) (Scanlon & Sahu, 2008; Scanlon & Kustas, 2010, 2012; Scanlon et al., 2019). Readers may refer to Text S1 in Supplementary Information and references therein for the mathematical formulation of FVS theory. The method has shown promising results in different land cover settings (Wagle et al., 2020; Wagle, Gowda, et al., 2021; Sulman et al., 2016; Scanlon & Kustas, 2012; L. Wang et al., 2010; W. Wang et al., 2016; Rana et al., 2018; Peddinti & Kambhammettu, 2019), including cropped systems such as rainfed alfalfa field (Wagle et al., 2020), Mediterranean cropping system (Rana et al., 2018), wheat (a C3 crop) (Scanlon & Sahu, 2008), corn (a C4 crop) (Scanlon & Kustas, 2010), and several others (Wagle, Skaggs, et al., 2021). One of the critical inputs to FVS method is the leaf-scale WUE. In the absence of direct measurements, leaf-scale WUE can be estimated as below:

$$WUE = \left(\frac{1}{DR}\right) \cdot \left(\frac{c_a - c_i}{q_a - q_i}\right) \tag{2}$$

where DR (=1.6) is the ratio of molecular diffusivities for water and carbon concentrations through the stomatal aperture (Massman, 1998). c_a (q_a) and c_i (q_i) are the ambient and intercellular concentrations of carbon (water), respectively. Here, c_a and q_a can be derived by extrapolating the logarithmic mean profile of EC measurements of carbon dioxide and water vapor fluxes with stability correction to zero displacement height (Scanlon & Sahu, 2008; Brutsaert, 2013). q_i is usually estimated assuming 100% relative humidity at leaf temperature (approximated as ±2 °C of the air temperature). c_i can be modeled in different ways in Fluxpart (Wagle, Skaggs, et al., 2021). Based on the findings of Wagle, Skaggs, et al. (2021) for wheat, we choose a constant ratio method where c_i/c_a is assumed to be constant (K); with K = 0.7 for C3 plants (Sinclair et al., 1984) and K = 0.44 for C4 plants (Kim et al., 2006).

Water flux partitioning based on uWUE concept was proposed by Zhou et al. (2016). Here in, partitioning is performed based on uWUE, which is obtained using Gross Primary Productivity (GPP) and Vapor Pressure Deficit (VPD) based on Zhou et al. (2014):

$$uWUE = \frac{GPP \cdot \sqrt{VPD}}{ET} \tag{3}$$

T:ET is estimated as:

$$\frac{T}{ET} = \frac{uWUE_a}{uWUE_p} \tag{4}$$

where $uWUE_a$ is the apparent $uWUE$ and $uWUE_p$ is the potential $uWUE$. $uWUE_a$ is estimated directly from Equation 3 if partitioning needs to be obtained at half-hour resolution. For estimates at coarser resolution (say a week or coarser), a linear regression between $GPP{\cdot}\sqrt{VPD}$ and ET is obtained using data derived through averaging of participating variables using a moving window approach. $uWUE_p$ represents the maximum carbon gain to water loss and is estimated using 95^{th} quantile regression between $GPP{\cdot}\sqrt{VPD}$ and ET for a given year or season. The key assumption of $uWUE$-based method is that $uWUE_p$ is constant for a given year or season and calculation of $uWUE_p$ is based on periods when $T \approx ET$ or $E \approx 0$. $uWUE$-based method is very straightforward in nature and easy to use. This approach has been used to partition water fluxes in different biomes (Zhou et al., 2016; Bai et al., 2019; Zhou et al., 2018; Xu et al., 2021; J.-y. Sun et al., 2020; H. Hu et al., 2018; Nelson et al., 2020).

TEA method is a nonlinear machine learning method for water flux partitioning Nelson et al. (2018). TEA method predicts the T using a Random Forest (RF) regressor which is trained for ecosystem WUE ($= GPP/ET$) during dry periods of growing season i.e., during periods when $E \approx 0$ or in other words the RF model is trained for GPP/T. The dry periods are selected by filtering out the wet periods from the time series based on rainfall and ET inputs. To ensure the good quality data for training the model, various quality control steps are performed, as detailed in Nelson et al. (2018). The trained model on the filtered data is then used to predict GPP/T for the full time series. TEA method has been shown to perform well across different ecosystems (Nelson et al., 2018, 2020; Räsänen et al., 2020; X. Hu & Lei, 2021; Migliavacca et al., 2021).

2.4 Modeling T:ET ratio

Partitioning using all three methods was performed for two growing seasons (2016-17 and 2017-18) at three wheat sites. The three partitioning methods have different data requirements to model T:ET. Partitioning from FVS method was performed using 10 Hz frequency EC data using Fluxpart version 0.2.10 (Skaggs et al., 2018). Partitioning from uWUE and TEA methods were done using the 30 minute interval flux data, which was obtained by processing high frequency EC data in EddyPro software (Wagle et al., 2018). The flux data was also processed with CO_2 flux partitioning (i.e., NEE to GPP and ecosystem respiration (R_{eco})) and gap filling using REddyProc package in R (Wutzler et al., 2018; Reichstein et al., 2005). Partition estimates were obtained at 30 minute interval using all three methods. Fluxpart may fail to produce outputs for a certain intervals because of various physical constraints (Scanlon et al., 2019; Palatella et al., 2014; Wagle, Skaggs, et al., 2021). Other two methods may also produce erroneous values of T:ET for certain time periods. We only used reliable estimates of T:ET, and filtered out the bad quality estimates following the rubric detailed in (Zhou et al., 2016; Nelson et al., 2018). Also, the hours with rainfall were removed from the analysis as partitioning estimates during it are expected to be unreliable. To obtain T:ET at weekly and monthly scales, weekly mean diurnal cycles were used. For example, to calculate the T:ET for a particular week, mean diurnal variations of T and ET at half-hour resolution were generated for the week, and then T:ET was determined by summing half-hourly binned mean T and mean ET. The resultant weekly average T:ET (a constant ratio for a week) was used to partition EC-measured daily ET values into daily E and T values.

3 Results and Discussion

3.1 Temporal variations in T:ET

Weekly T:ET ratios were obtained for all three wheat sites for 2016-2018 using the three ET partitioning methods (see Figures 1, S3, and S4). ET fluxes were larger during the 2016-17 growing season than the 2017-18 growing season at each site, in part because the former received much more rainfall. For example, total seasonal ET, i.e., ET during Nov-May in 2016-17 (2017-18) for grain-only and graze-grain wheat were ∼460 mm (∼345 mm) and ∼367 mm (∼287 mm), respectively. Corresponding precipitation totals for the two seasons were 501 mm and 155 mm, respectively. Notably, the change in T:ET between the two seasons was modest with its magnitude being 0.71 (0.74) and 0.70 (0.7) in grain-only and graze-grain wheat in 2016-17 (2017-18) based on FVS method. Corresponding seasonal T:ET estimates using uWUE method were 0.58 (0.58) and 0.54 (0.55) in grain-only and graze-grain wheat. TEA method yielded seasonal T:ET of 0.80 (0.78) and 0.74 (0.76). The small difference in T:ET across the two years and wheat systems is consistent with the findings of past studies (Good et al., 2017; Nelson et al., 2020; Wagle, Gowda, et al., 2021), which attribute it to the reduction in canopy cover when faced with limiting resources, and to the compensating effect of E from wet canopies (intercepted rainfall) vs. that from wet soil with changes in canopy cover. The T:ET was, however, found to be highly variable within the season (Figure 1) with weekly mean and coefficient of variation being 0.63 (0.67) and 13.95% (20.33%), respectively, in 2016-17 (2017-18) at the grain-only site for T:ET estimates from FVS method. The corresponding values for the graze-grain site were 0.62 (0.66) and 14.95% (14.45%). The intra-seasonal variations are attributable to a variety of hydroclimatic variables (e.g., rainfall, atmospheric water demand, available energy, and soil moisture). VPD, especially, had a strong control on T:ET variations with low T:ET values at low VPD and high values at high VPD. For example, average T:ET in grain-only wheat was 0.52 for low VPD values (VPD less than 25^{th} percentile) and T:ET was 0.84 for high VPD values (VPD larger than 75^{th} percentile). Increased soil wetness, coupled with low VPD, during and right-after the rain events also diminishes T:ET (X. Sun et al., 2019). For example, T:ET was around 0.52 during rainy days as compared to 0.70 during non-rainy days in January 2017 (EVI is low during this period) for grain-only system. This is true even for peak wheat growth period (Mid-March, 2017 to Mid-April, 2017; EVI is high during this period) when T:ET was about 0.64 during rainy days as compared to 0.82 during non-rainy days.

Intercomparison of all the three methods for ET partitioning shows that there is agreement among the methods in regards to capturing the overall temporal pattern of T:ET, with a correlation of 0.58 between FVS and TEA, 0.70 between FVS and uWUE, and 0.68 between TEA and uWUE (Figure 2). Overall, uWUE method underestimated the T:ET (with average T:ET=0.54) as compared to T:ET estimates from FVS method (with average T:ET=0.75), while the TEA method was in good agreement (with average T:ET=0.76) with FVS method. These results for TEA and uWUE are in agreement with Nelson et al. (2020) where uWUE method also produced lower T:ET estimates as compared to the TEA method.

3.2 Relation between T:ET and EVI

Following the lead of previous studies that reported a power-law relation between T:ET and vegetation indices (Wei et al., 2017; L. Wang et al., 2014; Wei et al., 2015; Lian et al., 2018), we derived such a relation $T : ET = aEVI^b$ between Landsat-derived EVI and average of weekly T:ET from all the ET partitioning methods in all three wheat systems, i.e., grain-only, graze-grain, and graze-out. As also done in the previous study, grouping of T:ET based on binning is performed to reduce the effects of confounding variables (e.g., rainfall, available energy) on the emergent T:ET-EVI relation during the growing period. Best fit parameters a and b for each system were found by performing a non-linear regression analysis using Nonlinear Least Squares (NLS) method in R (Bates & Watts, 1988; Elzhov et al., 2010). We found that the EVI could explain most of the variability (44-78%) in T:ET in grain-only wheat (Figure 3a, 3d, and 3g). This is consistent with other studies (Wei et al., 2017; Zhou et al., 2016; S. Kang et al., 2003) that reported a very strong positive correlation between vegetation indices and T:ET. However, this relationship was not strong for graze-grain and graze-out wheat systems (Figure 3). In the following section, we explore this aspect in more detail.

3.3 Errors in the prediction of T:ET using EVI

The applicability of previously reported canonical relations between EVI and T:ET for crop systems is first assessed in both disturbed (i.e.,grazed) and undisturbed (i.e., non-grazed) systems. To this end, the global crop relation ($T : ET = 0.66LAI^{0.18}$) presented in (Wei et al., 2017) is used. LAI was obtained from EVI based on Y. Kang et al. (2016). Results (Figure 4d) show that Mean Absolute Percentage Error (MAPE) or the ratio of absolute difference between predicted and observed T:ET, was significantly worse for disturbed systems at both weekly and monthly scales. Notably, the errors are larger (Figures 4a, 4b, and 4c) even when the T:ET vs. EVI relations derived at the neighboring undisturbed site is used from all the methods. For example, at weekly scale, MAPE was highest (about 20%) for graze-grain case and lowest (about 9%) for grain-only case (Figure 4). Similar results were also observed at monthly scales. We also evaluated the errors in each wheat system when using T:ET-EVI relations obtained in a differently managed system (see Table 1). Errors generally increased, with a few exceptions, when the T:ET-EVI relation developed for a wheat system is used for other at both weekly and monthly scales. Although the three sites are all winter wheat systems that experience similar hydroclimatology, the difference in management implementations make them act differently in regards to T:ET dynamics vis-a-vis EVI. Among the different temporal scales, errors were minimum at the seasonal scale. Smaller error at the seasonal scale is consistent with other studies which reported that T:ET are uncorrelated with vegetation growth across sites (Nelson et al., 2020; Fatichi & Pappas, 2017).

We further investigated the possible causes for the lack of strong relation between T:ET and EVI in graze-grain and graze-out systems. At ecosystem-scale, T rate is controlled by meteorological conditions, the stomatal conductance (g_s), and plant's biophysical state (e.g., LAI, EVI, etc.). T is usually proportional to $g_s \times LAI$. g_s is affected by multiple environmental variables, including VPD, soil moisture, radiation, and air temperature (Jarvis, 1976; Daly et al., 2004). Given our earlier result that showed a strong influence of VPD on T:ET (in section 3.1), we started with a hypothesis that the increase in T:ET with EVI in undisturbed systems is strongly influenced by the covariation of VPD and EVI. Any disturbance or grazing management may, however, disturb the covariation of EVI with VPD, thus also impacting the covariation of T:ET with EVI. To test this hypothesis, we obtained relations between EVI and T:ET for 10,000 different sample sets of randomly distributed 30 days from the growing season (Figure 5a) in the

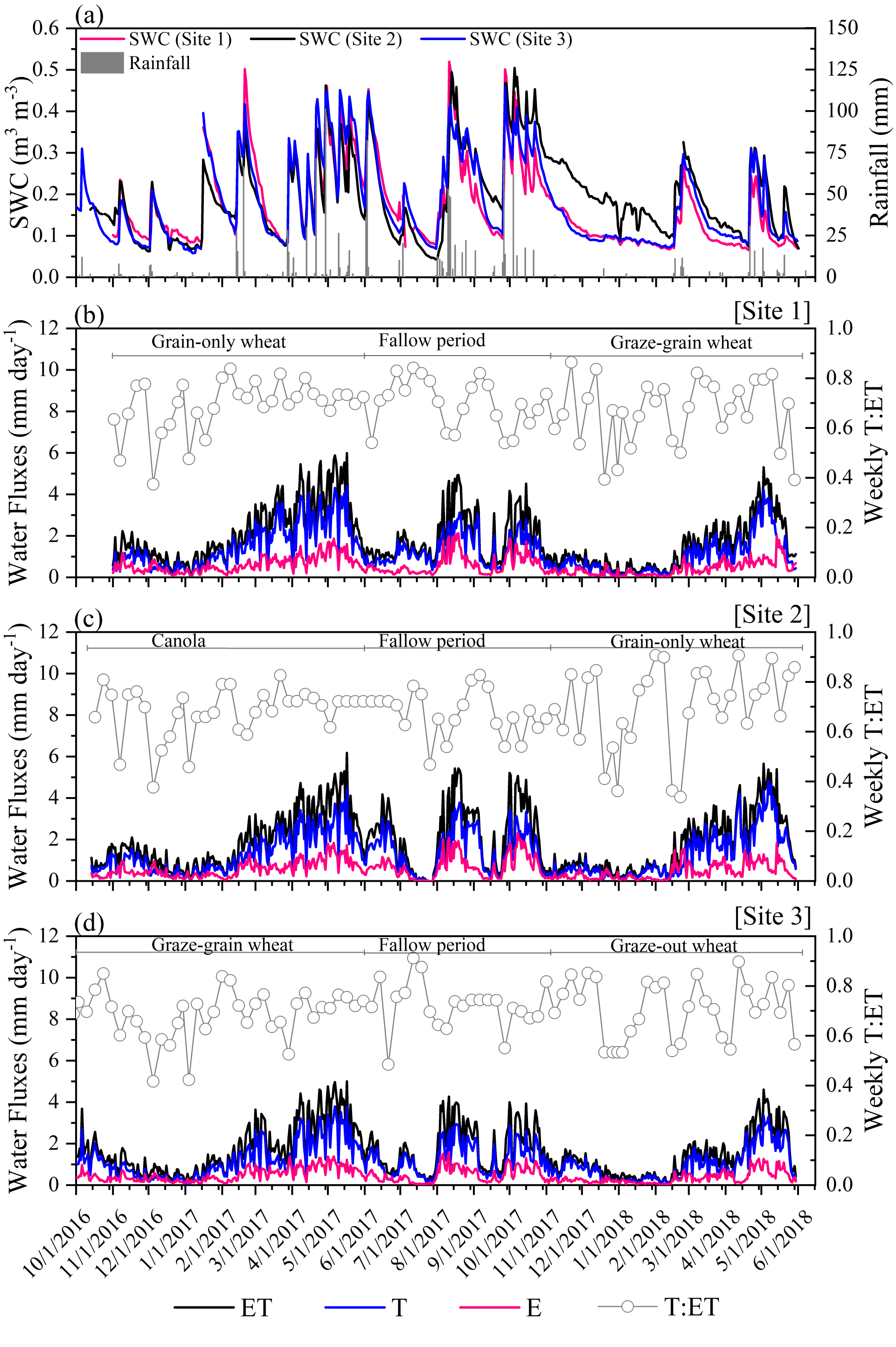

Figure 1. (a) Daily variations of rainfall and soil water content (SWC) at each site, (b) -(d) daily variations of total evapotranspiration (ET), transpiration (T), and direct evaporation (E) based on FVS method at three different sites. Open circles plotted on the secondary Y-axis show the ratio of weekly T and ET. Notably, all three sites underwent crop rotation. Fallow period and canola were not considered for analyses in this study.

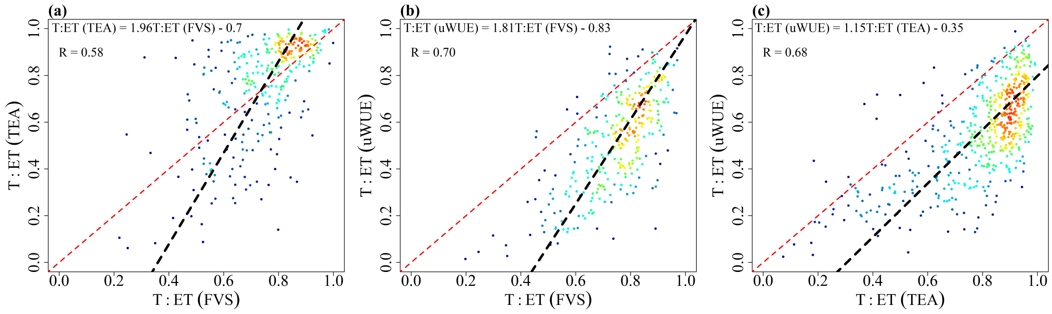

Figure 2. Intercomparison of the three ET partitioning methods, viz. T:ET (FVS) to T:ET (TEA) (a), T:ET (FVS) to T:ET (uWUE) (b), and T:ET (TEA) to T:ET (uWUE) (c), at daily temporal resolution for the three sites. R represents the Pearson correlation coefficient. The black dashed lines are the best fit linear lines estimated using orthogonal-least-squares regression (S. Chen et al., 1989). Notably, the data used for intercomparison only includes the period during which T:ET estimates are available for both the intercomparing methods. Colors of the data points represent the relative point density with warmer colors indicating higher density.

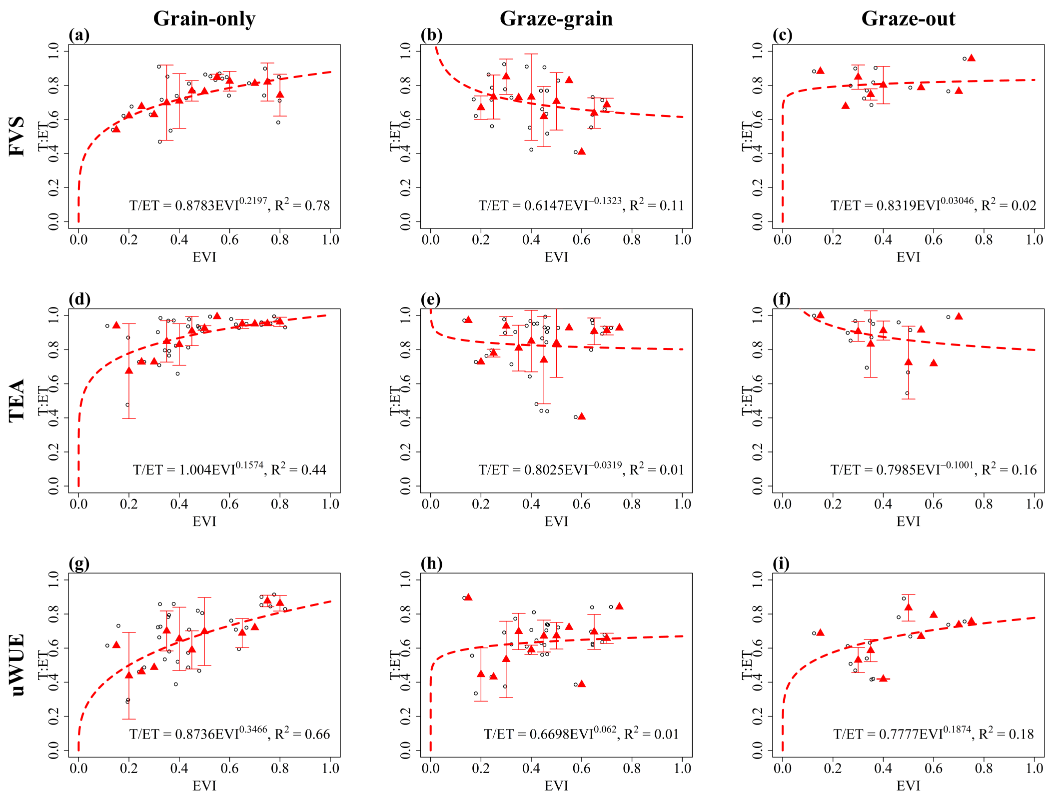

Figure 3. Relations between T:ET and EVI in differently managed winter wheat systems using the three ET partitioning methods; FVS (a)-(c), TEA (d)-(f), and uWUE (g)-(i). Grey dots are weekly T:ET, ±3 days around the Landsat image acquisition date, during mid-day (11AM-2PM). Red triangles are averaged T:ET corresponding to 0.05-bin EVI. The vertical lines are the error bars of mean T:ET for each bin. The red dash line in each panel is the best nonlinear fit between triangles and corresponding EVI.

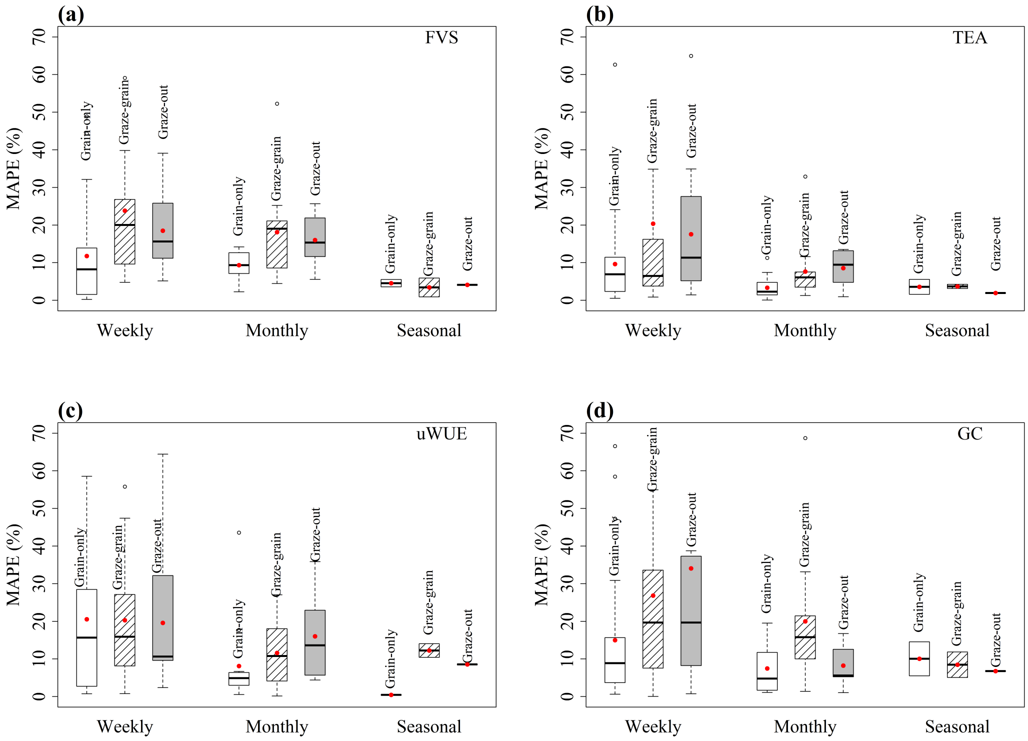

Figure 4. Mean Absolute Percentage Error (MAPE) of predicted T:ET using the relations developed in unmanaged system from FVS method (a), TEA method (b), and uWUE method (c) at weekly, monthly, and seasonal time scales for winter wheat systems with varied management implementations. An additional evaluation is performed using a relation (hereafter referred as GC) derived using global data over varied crops Wei et al. (2017) (d) Red dots represent the average MAPE.

Table 1. Average Mean Absolute Percentage Error (MAPE) (%) when using T:ET-EVI relations obtained in different wheat systems and the global crop relation presented in Wei et al. (2017). Here, G represents grain-only wheat system, GG represents graze-grain wheat system, GO represents graze-out wheat system, and GC represents the global crop relation.

T:ET-EVI relation	MAPE (%)								
	Weekly			Monthly			Seasonal		
	G	GG	GO	G	GG	GO	G	GG	GO
FVS (G)	11.76	23.84	18.50	9.33	18.12	16.01	4.55	3.42	4.09
FVS (GG)	20	17.67	12.1	15.97	15.53	9.23	2.61	2.04	2.67
FVS (GO)	19.16	32.54	8.96	8.36	20.91	7.92	15.43	13.55	12.75
TEA (G)	9.62	22.36	17.56	3.34	7.66	8.56	3.58	3.70	1.94
TEA (GG)	14.51	21.44	15.62	10.95	8.71	9.33	8.3	5.29	4.29
TEA (GO)	15.26	21.42	14.11	9.94	8.60	6.07	3.16	0.40	1.64
uWUE (G)	20.55	20.27	19.57	8.13	11.59	16.01	0.45	12.23	8.55
uWUE (GG)	27.65	30.13	26.58	29.54	26.98	30.87	29.61	27.54	26.97
uWUE (GO)	23.57	28.88	25.67	26.0	24.13	28.93	26.79	25.08	24.78
GC	14.99	26.84	34.06	7.46	20.00	8.24	10.04	8.47	6.77

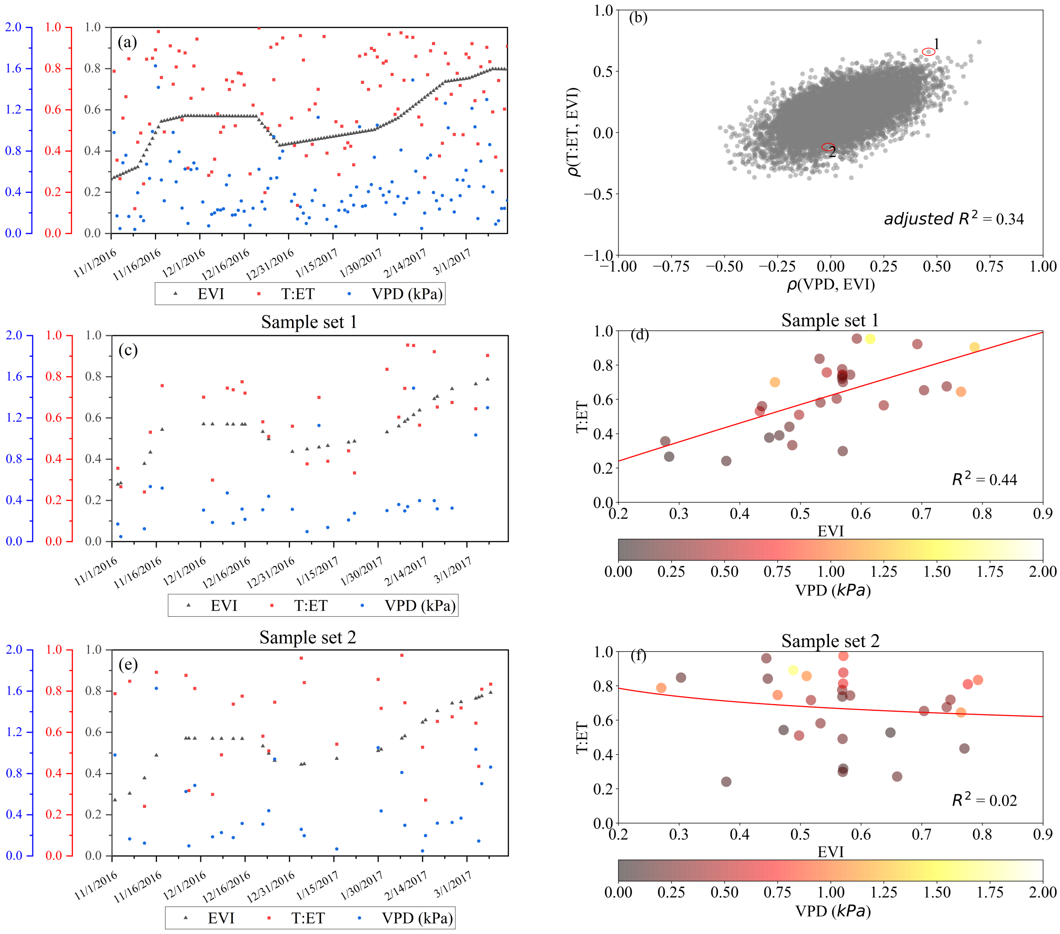

Figure 5. Temporal variations of EVI, T:ET, and VPD for all days (a), sample set 1 (c), and sample set 2 (e). Scatter of correlation between VPD and EVI and correlation between T:ET and EVI for 10000 sample sets with each set having randomly selected 30 days (b). Scatter between T:ET and EVI for sample set 1 (d) and sample set 2 (f). Red solid lines in panels d and f represent the best-fit nonlinear lines.

undisturbed system. Each set covers a wide enough range of EVI that is experienced in grain-only and graze-grain systems. The orientation of the point cloud along 1:1 direction in Figure 5b confirms that the relation between EVI and T:ET is stronger with higher correlation between VPD and EVI. To parse this further, we selected two sample sets with contrasting correlations between T:ET and EVI. Sample set 1 has ρ(T:ET, EVI) of 0.66 and sample set 2 has ρ(T:ET, EVI) of -0.12. Here ρ is the coefficient of correlation. The results suggest that if EVI is not co-varying closely with VPD (sample set 2, see Figure 5e), then the relation between T:ET and EVI is not strong (Figure 5f). But if EVI co-varies closely with VPD, then the T:ET-EVI relation improves (see Figures 5c&5d). In fact, at the unmanaged site where a strong T:ET-EVI relation is obtained (see Figure 1), the correlation between VPD and EVI until the peak growth period is 0.60. In contrast, the corresponding value for graze-grain and graze-out cases were 0.15 and -0.36, respectively. Similar evaluations were also conducted for uWUE (see Figure S8 in Supplementary Information) method and TEA method (see Figure S9 in Supplementary Information). Furthermore, evaluations were also conducted for soil moisture, radiation, and air temperature, variables known to affect the stomatal conductance (see Figures S5-S7 in Supplementary Information). Results indicate that the covariation of solar radiation with EVI also explained the covariation of T:ET with EVI, although the relation was less stronger. The influences of air temperature and soil moisture were much less (see Figures S6-S7 in Supplementary Information).

4 Conclusions

Using T:ET-EVI relations, ET partitioning was performed in winter wheat systems with varied grazing management schemes. Comparison with partitioning estimates obtained based on three ET partitioning methods, viz. flux variance similarity theory, underlying Water Use Efficiency, and Transpiration Estimation Algorithm, all indicate a robust T:ET-EVI relation in a standard undisturbed system. In contrast, the relation in disturbed systems, realized by cattle grazing in this case, is weak and do not capture the data variance well. The results indicate that the relation between vegetation indices and T:ET is affected by canopy alterations, which in this study was due to grazing management but could also be a result of other natural (e.g., fire or drought) or anthropogenic (e.g., thinning) disturbances. In addition, our results show prediction of T:ET at weekly to monthly scale using the T:ET-EVI relation of undisturbed systems in disturbed system introduces large errors. As prediction of T:ET using data from disturbed system in an undisturbed system and vice-versa introduces uncertainty in T:ET estimates, the results point to limited translatability of the method across systems. Given that more than 40% of the global land is managed or disturbed (Ellis et al., 2010), the results underscore the need for caution while assessing ET partitioning using vegetation indices over managed or disturbed systems. Notably, the impact of grazing management on T:ET estimate at the seasonal scale is negligible. This is attributable to plants' adaptation to the given water resources and the compensatory effects of E from wet canopies and wet soil surfaces under contrasting (dense and sparse) canopies.

Investigation on the possible causes of the altered T:ET-EVI relation suggest that grazing disturbed the co-variation of EVI and VPD (and of EVI and solar radiation), resulting in divergence from the standard T:ET-EVI relation. As the covariation between VPD (or solar radiation) and EVI can be easily evaluated using global meteorological forcings (Weedon et al., 2014; Xia et al., 2012; Mooney et al., 2011; Warszawski et al., 2014) and vegetation (Hatfield & Prueger, 2010; Benedetti & Rossini, 1993; Huete et al., 2002, 1994; Jiang et al., 2008; Rocha & Shaver, 2009; Nguyen et al., 2020) data, future studies may use this metric, after further assessments in alternative settings, to map regions where vegetation indices are likely to be effective for ET partitioning.

Acknowledgments

This work is partially supported by NSF OIA-2019561, NSF EAR-1920425, and NSF EAR-1856054. Partial funding supports from the USDA-ARS Office of National Programs (Project number: 3070-21610-003-00D), USDA-ARS Long-Term Agroecosystem Research Network, and USDA-NIFA's research grant (Project No. 2019-68012-29888) are also acknowledged. Authors thank developers of the Fluxpart source code, which is accessible at `https://github.com/usda-ars-ussl/fluxpart` (accessed on November 10, 2020). The code for TEA algorithm is available at `https://doi.org/10.5281/zenodo.3921923`.The code for uWUE algorithm is available at `https://github.com/praghav444/WaterFluxPartitioning`. Data are uploaded as Supporting Information for review. Readers can access the data from one of the repositories by acceptance.

References

Alkama, R., & Cescatti, A. (2016). Biophysical climate impacts of recent changes in global forest cover. *Science*, *351*(6273), 600–604.

Bai, Y., Li, X., Zhou, S., Yang, X., Yu, K., Wang, M., ... others (2019). Quantifying plant transpiration and canopy conductance using eddy flux data: An underlying water use efficiency method. *Agricultural and Forest Meteorology*, *271*, 375–384.

Bates, D. M., & Watts, D. G. (1988). *Nonlinear regression analysis and its applications* (Vol. 2). Wiley New York.

Benedetti, R., & Rossini, P. (1993). On the use of ndvi profiles as a tool for agricultural statistics: the case study of wheat yield estimate and forecast in emilia romagna. *Remote Sensing of Environment*, *45*(3), 311–326.

Berkelhammer, M., Noone, D., Wong, T., Burns, S., Knowles, J., Kaushik, A., ... Williams, M. (2016). Convergent approaches to determine an ecosystem's transpiration fraction. *Global Biogeochemical Cycles*, *30*(6), 933–951.

Black, T., Gardner, W., & Thurtell, G. (1969). The prediction of evaporation, drainage, and soil water storage for a bare soil. *Soil Science Society of America Journal*, *33*(5), 655–660.

Bonetti, S., Manoli, G., Domec, J.-C., Putti, M., Marani, M., & Katul, G. G. (2015). The influence of water table depth and the free atmospheric state on convective rainfall predisposition. *Water Resources Research*, *51*(4), 2283–2297.

Brutsaert, W. (2013). *Evaporation into the atmosphere: theory, history and applications* (Vol. 1). Springer Science & Business Media.

Chen, S., Billings, S. A., & Luo, W. (1989). Orthogonal least squares methods and their application to non-linear system identification. *International Journal of control*, *50*(5), 1873–1896.

Chen, X., Kumar, M., & McGlynn, B. L. (2015). Variations in streamflow response to large hurricane-season storms in a southeastern us watershed. *Journal of Hydrometeorology*, *16*(1), 55–69.

Condon, L. E., & Maxwell, R. M. (2019). Simulating the sensitivity of evapotranspiration and streamflow to large-scale groundwater depletion. *Science Advances*, *5*(6), eaav4574.

Daly, E., Porporato, A., & Rodriguez-Iturbe, I. (2004). Coupled dynamics of photosynthesis, transpiration, and soil water balance. part i: Upscaling from hourly to daily level. *Journal of Hydrometeorology*, *5*(3), 546–558.

Dirmeyer, P. A., Gao, X., Zhao, M., Guo, Z., Oki, T., & Hanasaki, N. (2006). Gswp-2: Multimodel analysis and implications for our perception of the land surface. *Bulletin of the American Meteorological Society*, *87*(10), 1381–1398.

Ellis, E. C., Klein Goldewijk, K., Siebert, S., Lightman, D., & Ramankutty, N. (2010). Anthropogenic transformation of the biomes, 1700 to 2000. *Global ecology and biogeography*, *19*(5), 589–606.

Elzhov, T. V., Mullen, K. M., Spiess, A., & Bolker, B. (2010). R interface to the levenberg-marquardt nonlinear least-squares algorithm found in minpack. *Plus support for bounds*, 1–2.

Fatichi, S., & Pappas, C. (2017). Constrained variability of modeled t: Et ratio across biomes. *Geophysical Research Letters*, *44*(13), 6795–6803.

Good, S. P., Moore, G. W., & Miralles, D. G. (2017). A mesic maximum in biological water use demarcates biome sensitivity to aridity shifts. *Nature ecology & evolution*, *1*(12), 1883–1888.

Good, S. P., Noone, D., & Bowen, G. (2015). Hydrologic connectivity constrains partitioning of global terrestrial water fluxes. *Science*, *349*(6244), 175–177.

Haddeland, I., Clark, D. B., Franssen, W., Ludwig, F., Voß, F., Arnell, N. W., ... others (2011). Multimodel estimate of the global terrestrial water balance: Setup and first results. *Journal of Hydrometeorology*, *12*(5), 869–884.

Hatfield, J. L., & Prueger, J. H. (2010). Value of using different vegetative indices to quantify agricultural crop characteristics at different growth stages under varying management practices. *Remote Sensing*, *2*(2), 562–578.

Hu, H., Chen, L., Liu, H., Ali Khan, M. Y., Tie, Q., Zhang, X., & Tian, F. (2018). Comparison of the vegetation effect on et partitioning based on eddy covariance method at five different sites of northern china. *Remote sensing*, *10*(11), 1755.

Hu, X., & Lei, H. (2021). Evapotranspiration partitioning and its interannual variability over a winter wheat-summer maize rotation system in the north china plain. *Agricultural and Forest Meteorology*, *310*, 108635.

Huete, A., Didan, K., Miura, T., Rodriguez, E. P., Gao, X., & Ferreira, L. G. (2002). Overview of the radiometric and biophysical performance of the modis vegetation indices. *Remote sensing of environment*, *83*(1-2), 195–213.

Huete, A., Justice, C., & Liu, H. (1994). Development of vegetation and soil indices for modis-eos. *Remote Sensing of environment*, *49*(3), 224–234.

Jarvis, P. (1976). The interpretation of the variations in leaf water potential and stomatal conductance found in canopies in the field. *Philosophical Transactions of the Royal Society of London. B, Biological Sciences*, *273*(927), 593–610.

Jasechko, S., Sharp, Z. D., Gibson, J. J., Birks, S. J., Yi, Y., & Fawcett, P. J. (2013). Terrestrial water fluxes dominated by transpiration. *Nature*, *496*(7445), 347–350.

Jiang, Z., Huete, A. R., Didan, K., & Miura, T. (2008). Development of a two-band enhanced vegetation index without a blue band. *Remote sensing of Environment*, *112*(10), 3833–3845.

Jung, M., Reichstein, M., Ciais, P., Seneviratne, S. I., Sheffield, J., Goulden, M. L., ... others (2010). Recent decline in the global land evapotranspiration trend due to limited moisture supply. *Nature*, *467*(7318), 951–954.

Kang, S., Gu, B., Du, T., & Zhang, J. (2003). Crop coefficient and ratio of transpiration to evapotranspiration of winter wheat and maize in a semi-humid region. *Agricultural water management*, *59*(3), 239–254.

Kang, Y., Özdoğan, M., Zipper, S. C., Román, M. O., Walker, J., Hong, S. Y., ... others (2016). How universal is the relationship between remotely sensed vegetation indices and crop leaf area index? a global assessment. *Remote sensing*, *8*(7), 597.

Kim, S.-H., Sicher, R. C., Bae, H., Gitz, D. C., Baker, J. T., Timlin, D. J., & Reddy, V. R. (2006). Canopy photosynthesis, evapotranspiration, leaf nitrogen, and transcription profiles of maize in response to co2 enrichment. *Global Change Biology*, *12*(3), 588–600.

Kool, D., Agam, N., Lazarovitch, N., Heitman, J., Sauer, T., & Ben-Gal, A. (2014). A review of approaches for evapotranspiration partitioning. *Agricultural and forest meteorology*, *184*, 56–70.

Li, X., Gentine, P., Lin, C., Zhou, S., Sun, Z., Zheng, Y., ... Zheng, C. (2019). A simple and objective method to partition evapotranspiration into transpiration and evaporation at eddy-covariance sites. *Agricultural and Forest Meteorology*, *265*, 171–182.

Lian, X., Piao, S., Huntingford, C., Li, Y., Zeng, Z., Wang, X., … others (2018). Partitioning global land evapotranspiration using cmip5 models constrained by observations. *Nature Climate Change*, *8*(7), 640–646.

Liu, Y., Kumar, M., Katul, G. G., Feng, X., & Konings, A. G. (2020). Plant hydraulics accentuates the effect of atmospheric moisture stress on transpiration. *Nature Climate Change*, *10*(7), 691–695.

Liu, Y., Parolari, A. J., Kumar, M., Huang, C.-W., Katul, G. G., & Porporato, A. (2017). Increasing atmospheric humidity and co2 concentration alleviate forest mortality risk. *Proceedings of the National Academy of Sciences*, *114*(37), 9918–9923.

Long, D., & Singh, V. P. (2012). A two-source trapezoid model for evapotranspiration (ttme) from satellite imagery. *Remote Sensing of Environment*, *121*, 370–388.

Martens, B., Miralles, D. G., Lievens, H., Van Der Schalie, R., De Jeu, R. A., Fernández-Prieto, D., … Verhoest, N. E. (2017). Gleam v3: Satellite-based land evaporation and root-zone soil moisture. *Geoscientific Model Development*, *10*(5), 1903–1925.

Massman, W. (1998). A review of the molecular diffusivities of h2o, co2, ch4, co, o3, so2, nh3, n2o, no, and no2 in air, o2 and n2 near stp. *Atmospheric environment*, *32*(6), 1111–1127.

Migliavacca, M., Musavi, T., Mahecha, M. D., Nelson, J. A., Knauer, J., Baldocchi, D. D., … others (2021). The three major axes of terrestrial ecosystem function. *Nature*, *598*(7881), 468–472.

Miralles, D. G., Holmes, T., De Jeu, R., Gash, J., Meesters, A., & Dolman, A. (2011). Global land-surface evaporation estimated from satellite-based observations. *Hydrology and Earth System Sciences*, *15*(2), 453–469.

Mooney, P. A., Mulligan, F. J., & Fealy, R. (2011). Comparison of era-40, era-interim and ncep/ncar reanalysis data with observed surface air temperatures over ireland. *International Journal of Climatology*, *31*(4), 545–557.

Nelson, J. A., Carvalhais, N., Cuntz, M., Delpierre, N., Knauer, J., Ogée, J., … Jung, M. (2018). Coupling water and carbon fluxes to constrain estimates of transpiration: The tea algorithm. *Journal of Geophysical Research: Biogeosciences*, *123*(12), 3617–3632.

Nelson, J. A., Pérez-Priego, O., Zhou, S., Poyatos, R., Zhang, Y., Blanken, P. D., … others (2020). Ecosystem transpiration and evaporation: Insights from three water flux partitioning methods across fluxnet sites. *Global change biology*, *26*(12), 6916–6930.

Nguyen, L. H., Joshi, D. R., Clay, D. E., & Henebry, G. M. (2020). Characterizing land cover/land use from multiple years of landsat and modis time series: A novel approach using land surface phenology modeling and random forest classifier. *Remote Sensing of Environment*, *238*, 111017.

Oishi, A. C., Oren, R., Novick, K. A., Palmroth, S., & Katul, G. G. (2010). Interannual invariability of forest evapotranspiration and its consequence to water flow downstream. *Ecosystems*, *13*(3), 421–436.

Oki, T., & Kanae, S. (2006). Global hydrological cycles and world water resources. *science*, *313*(5790), 1068–1072.

Palatella, L., Rana, G., & Vitale, D. (2014). Towards a flux-partitioning procedure based on the direct use of high-frequency eddy-covariance data. *Boundary-layer meteorology*, *153*(2), 327–337.

Paschalis, A., Fatichi, S., Pappas, C., & Or, D. (2018). Covariation of vegetation and climate constrains present and future t/et variability. *Environmental Research Letters*, *13*(10), 104012.

Paul-Limoges, E., Wolf, S., Schneider, F. D., Longo, M., Moorcroft, P., Gharun, M.,

& Damm, A. (2020). Partitioning evapotranspiration with concurrent eddy covariance measurements in a mixed forest. *Agricultural and Forest Meteorology*, *280*, 107786.

Peddinti, S. R., & Kambhammettu, B. P. (2019). Dynamics of crop coefficients for citrus orchards of central india using water balance and eddy covariance flux partition techniques. *Agricultural Water Management*, *212*, 68–77.

Perez-Priego, O., Katul, G., Reichstein, M., El-Madany, T. S., Ahrens, B., Carrara, A., … Migliavacca, M. (2018). Partitioning eddy covariance water flux components using physiological and micrometeorological approaches. *Journal of Geophysical Research: Biogeosciences*, *123*(10), 3353–3370.

Rana, G., Palatella, L., Scanlon, T. M., Martinelli, N., & Ferrara, R. M. (2018). Co2 and h2o flux partitioning in a mediterranean cropping system. *Agricultural and Forest Meteorology*, *260*, 118–130.

Räsänen, M., Aurela, M., Vakkari, V., Beukes, J. P., Tuovinen, J.-P., Van Zyl, P. G., … others (2020). The effect of rainfall amount and timing on annual transpiration in grazed savanna grassland. *Hydrology and Earth System Sciences Discussions*, 1–31.

Reichstein, M., Falge, E., Baldocchi, D., Papale, D., Aubinet, M., Berbigier, P., … others (2005). On the separation of net ecosystem exchange into assimilation and ecosystem respiration: review and improved algorithm. *Global change biology*, *11*(9), 1424–1439.

Ritchie, J. T., & Burnett, E. (1971). Dryland evaporative flux in a subhumid climate: Ii. plant influences 1. *Agronomy Journal*, *63*(1), 56–62.

Rocha, A. V., & Shaver, G. R. (2009). Advantages of a two band evi calculated from solar and photosynthetically active radiation fluxes. *Agricultural and Forest Meteorology*, *149*(9), 1560–1563.

Scanlon, T. M., & Kustas, W. P. (2010). Partitioning carbon dioxide and water vapor fluxes using correlation analysis. *Agricultural and Forest Meteorology*, *150*(1), 89–99.

Scanlon, T. M., & Kustas, W. P. (2012). Partitioning evapotranspiration using an eddy covariance-based technique: Improved assessment of soil moisture and land–atmosphere exchange dynamics. *Vadose Zone Journal*, *11*(3).

Scanlon, T. M., & Sahu, P. (2008). On the correlation structure of water vapor and carbon dioxide in the atmospheric surface layer: A basis for flux partitioning. *Water Resources Research*, *44*(10).

Scanlon, T. M., Schmidt, D. F., & Skaggs, T. H. (2019). Correlation-based flux partitioning of water vapor and carbon dioxide fluxes: Method simplification and estimation of canopy water use efficiency. *Agricultural and Forest Meteorology*, *279*, 107732.

Scott, R. L., & Biederman, J. A. (2017). Partitioning evapotranspiration using long-term carbon dioxide and water vapor fluxes. *Geophysical Research Letters*, *44*(13), 6833–6840.

Sinclair, T. R., Tanner, C., & Bennett, J. (1984). Water-use efficiency in crop production. *Bioscience*, *34*(1), 36–40.

Skaggs, T. H., Anderson, R. G., Alfieri, J., Scanlon, T., & Kustas, W. (2018). Fluxpart: Open source software for partitioning carbon dioxide and water vapor fluxes. *Agricultural and Forest Meteorology*, *253*, 218–224.

Stoy, P. C., El-Madany, T. S., Fisher, J. B., Gentine, P., Gerken, T., Good, S. P., … others (2019). Reviews and syntheses: Turning the challenges of partitioning ecosystem evaporation and transpiration into opportunities. *Biogeosciences*, *16*(19), 3747–3775.

Sulman, B. N., Roman, D. T., Scanlon, T. M., Wang, L., & Novick, K. A. (2016). Comparing methods for partitioning a decade of carbon dioxide and water vapor fluxes in a temperate forest. *Agricultural and forest meteorology*, *226*, 229–245.

Sun, J.-y., Sun, X.-y., Hu, Z.-y., & Wang, G.-x. (2020). Exploring the influence of environmental factors in partitioning evapotranspiration along an elevation gradient on mount gongga, eastern edge of the qinghai-tibet platea, china. *Journal of Mountain Science*, *17*(2), 384–396.

Sun, X., Wilcox, B. P., & Zou, C. B. (2019). Evapotranspiration partitioning in dryland ecosystems: A global meta-analysis of in situ studies. *Journal of Hydrology*, *576*, 123–136.

Unkovich, M., Baldock, J., & Farquharson, R. (2018). Field measurements of bare soil evaporation and crop transpiration, and transpiration efficiency, for rainfed grain crops in australia–a review. *Agricultural water management*, *205*, 72–80.

Wagle, P., Gowda, P. H., Manjunatha, P., Northup, B. K., Rocateli, A. C., & Taghvaeian, S. (2019). Carbon and water dynamics in co-located winter wheat and canola fields in the us southern great plains. *Agricultural and Forest Meteorology*, *279*, 107714.

Wagle, P., Gowda, P. H., Northup, B. K., & Neel, J. P. (2021). Ecosystem-level water use efficiency and evapotranspiration partitioning in conventional till and no-till rainfed canola. *Agricultural Water Management*, *250*, 106825.

Wagle, P., Gowda, P. H., Northup, B. K., Turner, K. E., Neel, J. P., Manjunatha, P., & Zhou, Y. (2018). Variability in carbon dioxide fluxes among six winter wheat paddocks managed under different tillage and grazing practices. *Atmospheric Environment*, *185*, 100–108.

Wagle, P., Skaggs, T. H., Gowda, P. H., Northup, B. K., & Neel, J. P. (2020). Flux variance similarity-based partitioning of evapotranspiration over a rainfed alfalfa field using high frequency eddy covariance data. *Agricultural and Forest Meteorology*, *285*, 107907.

Wagle, P., Skaggs, T. H., Gowda, P. H., Northup, B. K., Neel, J. P., & Anderson, R. G. (2021). Evaluation of water use efficiency algorithms for flux variance similarity-based evapotranspiration partitioning in c3 and c4 grain crops. *Water Resources Research*, e2020WR028866.

Wang, H., & Liu, C. (2007). Soil evaporation and its affecting factors under crop canopy. *Communications in soil science and plant analysis*, *38*(1-2), 259–271.

Wang, L., Caylor, K. K., Villegas, J. C., Barron-Gafford, G. A., Breshears, D. D., & Huxman, T. E. (2010). Partitioning evapotranspiration across gradients of woody plant cover: Assessment of a stable isotope technique. *Geophysical Research Letters*, *37*(9).

Wang, L., Good, S. P., & Caylor, K. K. (2014). Global synthesis of vegetation control on evapotranspiration partitioning. *Geophysical Research Letters*, *41*(19), 6753–6757.

Wang, R., Kumar, M., & Marks, D. (2013). Anomalous trend in soil evaporation in a semi-arid, snow-dominated watershed. *Advances in water resources*, *57*, 32–40.

Wang, W., Smith, J. A., Ramamurthy, P., Baeck, M. L., Bou-Zeid, E., & Scanlon, T. M. (2016). On the correlation of water vapor and co2: application to flux partitioning of evapotranspiration. *Water Resources Research*, *52*(12), 9452–9469.

Warszawski, L., Frieler, K., Huber, V., Piontek, F., Serdeczny, O., & Schewe, J. (2014). The inter-sectoral impact model intercomparison project (isi–mip): project framework. *Proceedings of the National Academy of Sciences*, *111*(9), 3228–3232.

Weedon, G. P., Balsamo, G., Bellouin, N., Gomes, S., Best, M. J., & Viterbo, P. (2014). The wfdei meteorological forcing data set: Watch forcing data methodology applied to era-interim reanalysis data. *Water Resources Research*, *50*(9), 7505–7514.

Wei, Z., Yoshimura, K., Okazaki, A., Kim, W., Liu, Z., & Yokoi, M. (2015). Partitioning of evapotranspiration using high-frequency water vapor isotopic measurement over a rice paddy field. *Water Resources Research*, *51*(5), 3716–3729.

Wei, Z., Yoshimura, K., Wang, L., Miralles, D. G., Jasechko, S., & Lee, X. (2017). Revisiting the contribution of transpiration to global terrestrial evapotranspiration. *Geophysical Research Letters*, *44*(6), 2792–2801.

Wutzler, T., Lucas-Moffat, A., Migliavacca, M., Knauer, J., Sickel, K., Šigut, L., ... Reichstein, M. (2018). Basic and extensible post-processing of eddy covariance flux data with reddyproc. *Biogeosciences*, *15*(16), 5015–5030.

Xia, Y., Mitchell, K., Ek, M., Cosgrove, B., Sheffield, J., Luo, L., ... others (2012). Continental-scale water and energy flux analysis and validation for north american land data assimilation system project phase 2 (nldas-2): 2. validation of model-simulated streamflow. *Journal of Geophysical Research: Atmospheres*, *117*(D3).

Xu, Z., Zhu, Z., Liu, S., Song, L., Wang, X., Zhou, S., ... Xu, T. (2021). Evapotranspiration partitioning for multiple ecosystems within a dryland watershed: Seasonal variations and controlling factors. *Journal of Hydrology*, *598*, 126483.

Zeng, Z., Piao, S., Li, L. Z., Zhou, L., Ciais, P., Wang, T., ... others (2017). Climate mitigation from vegetation biophysical feedbacks during the past three decades. *Nature Climate Change*, *7*(6), 432–436.

Zhang, Y., Kong, D., Gan, R., Chiew, F. H., McVicar, T. R., Zhang, Q., & Yang, Y. (2019). Coupled estimation of 500 m and 8-day resolution global evapotranspiration and gross primary production in 2002–2017. *Remote Sensing of Environment*, *222*, 165–182.

Zhang, Y., Peña-Arancibia, J. L., McVicar, T. R., Chiew, F. H., Vaze, J., Liu, C., ... others (2016). Multi-decadal trends in global terrestrial evapotranspiration and its components. *Scientific reports*, *6*(1), 1–12.

Zhou, S., Yu, B., Huang, Y., & Wang, G. (2014). The effect of vapor pressure deficit on water use efficiency at the subdaily time scale. *Geophysical Research Letters*, *41*(14), 5005–5013.

Zhou, S., Yu, B., Zhang, Y., Huang, Y., & Wang, G. (2016). Partitioning evapotranspiration based on the concept of underlying water use efficiency. *Water Resources Research*, *52*(2), 1160–1175.

Zhou, S., Yu, B., Zhang, Y., Huang, Y., & Wang, G. (2018). Water use efficiency and evapotranspiration partitioning for three typical ecosystems in the heihe river basin, northwestern china. *Agricultural and Forest Meteorology*, *253*, 261–273.